

Challenges related to propulsor – ice interaction in arctic waters

Lasse Norhamo¹, Geir Magne Bakken², Oddvar Deinboll³, Johan Johansson Iseskär⁴

¹ & ⁴ Det Norske Veritas, Approval Centre Norway, Høvik, Norway

² Det Norske Veritas, Maritime Technology Consultancy, Høvik, Norway

³ Det Norske Veritas, Approval Centre for East Asia, Busan, Rep. of Korea

ABSTRACT

This paper addresses important aspects related to propulsor – ice interaction, based on past 20 year's research and rule development. Propeller – ice impact loads will normally originate from either a milling situation (the propeller blade edge cutting through the ice), ice crushing (ice is pressed onto propeller blade or another surface, until the crushing pressure of ice is reached), or a combination of the two. The direction of ice loads acting on the propeller blades depends on relative velocities between ice and propeller, and the ice loads will generate both axial and transverse forces generating bending- and spindle moments on the blades and torque on the propeller and consequent load responses into the shafting system.

The different physics of the ice load phenomena are presented. The paper explains how ice load distributions can be derived from extreme loads predicted according to described load models. Assessment of strength of propeller blades and pitch mechanism, and components in the propulsion line, are discussed. A brief discussion on the practical consequences of designing propulsion systems to the Polar Classes is included.

Keywords

Polar Class, DNV, Propulsor, Ice, Loading

1 INTRODUCTION AND HISTORY

During 1980ties it became increasingly evident that existing machinery ice strengthening regulations were inadequate to the task, and had in many areas become less relevant. For example, blade scantlings in the Baltic and Canadian rules were dependent upon a design ice torque, rather than a direct expression of the ice load on a blade, which can cause major blade deformation and breakage, or fatigue failure. Another example was cracking of blade tips and trailing edges on high skew CP-propeller blades (highly skewed FP propellers with high ice class are rare, due to very high ice loads during reversing, see also Ch. 2.4).

Already at the end of 1970ties Finnish and Swedish Marine Authorities had decided to update their respective ice regulations. At the end of the 1980ties the Canadian and Finnish and Swedish Marine Authorities had decided to share expertise and resources, and a Canada/Finland joint

research project arrangement JRPA#6 on the important matter of blade design ice loads, was entered into between Canada and Finland. Finland would develop a numerical simulation model of propeller and ice interaction during the ice milling operation, which would incorporate a Finnish model for contact load components and a Canadian model for non-contact load components. A number of associated research programmes provided additional information, such as ice properties at interaction velocities, and analysis of available full scale data.

IACS joined into the development of "Polar code" in mid 1990ties. Thus the dependencies in the load formulae, with some modifications based on Russian R&D results, find their way into the new IACS UR I3 (2006).

The numerical simulation model did not address the ducted propeller directly, nor maximum forward blade loads. However, it was possible to determine working formulations based on available full scale data.

2 PROPELLOR ICE LOAD SCENARIOS

2.1 Maximum backward blade force

The formula for the maximum backward blade ice force, F_{bi} (kN) on a propeller blade, derived from the JRPA#6 numerical simulation model, is given in Reference No 8 as:

$$F_b = 93.0 \left(\frac{\sigma EAR}{Z} \right)^{0.287} \left(\frac{H_i}{D} \right)^{1.36} e^{-0.183\alpha} (nD)^{0.712} D^{2.02} \quad (1)$$

Where D is propeller diameter (m), Z is number of blades (-), EAR is expanded blade area ratio (-), n is propeller rotational speed (rps), H_i is ice thickness (m), σ is uniaxial unconfined compressive strength of ice (N/mm^2) and α is apparent angle of attack (rad) = $\phi - \text{atan}(V/(0.7\pi nD))$, where V is inflow speed (m/s), and ϕ is pitch angle at 0.7R.

The blade force increase with increasing ratio of ice thickness/propeller diameter is limited due to two factors:

- As ice thickness and block size and inertia increase, the interaction moves towards the infinite ice block case, and the loads move asymptotically to a limiting value.
- As ice thickness increases to be greater than blade length, the interaction geometry becomes more asymmetric, and the ice block tends to rotate on

contact away from the blade, thereby releasing or limiting the load.

It was found that when $H_i/D > 0.65$, H_i/D could be limited to 0.65 for calculation purposes.

This blade force is known from full scale observations and measurements referred to in the “Propeller Ice Interaction Loads”, ref. 8 and laboratory tests [reference 4], to be distributed radially in a strip close to the blade leading edge, modelled as a homogenous pressure distributed radially from 0.6R to the tip. Chord-wise, the load is distributed over 20% of the chord length back from the leading edge. This formula was further developed to “regulatory use” and several simplifications were introduced. Among others following:

- Ice strength index “ S_{ice} ” replaces compressive ice strength in three steps
- Angle of attack $+4^\circ$ was selected (See also Ch.3)

Backward load, F_b (kN) formula in “IACS (2006)” reads:

When $D < D_{limit} = 0.85 (H_{ice})^{1.4}$:

$$F_b = 27 S_{ice} (nD)^{0.7} \left(\frac{EAR}{Z} \right)^{0.3} D^2 \quad (2)$$

When $D > D_{limit}$:

$$F_b = 23 S_{ice} (nD)^{0.7} \left(\frac{EAR}{Z} \right)^{0.3} H_{ice}^{1.4} D \quad (3)$$

Table 1, Ice class parameters

Ice Class	H_{ice} (m)	S_{ice} (-)
PC1	4.0	1.2
PC2	3.5	1.1
PC3	3.0	1.1
PC4	2.5	1.1
PC5	2.0	1.1
PC6	1.75	1
PC7	1.5	1

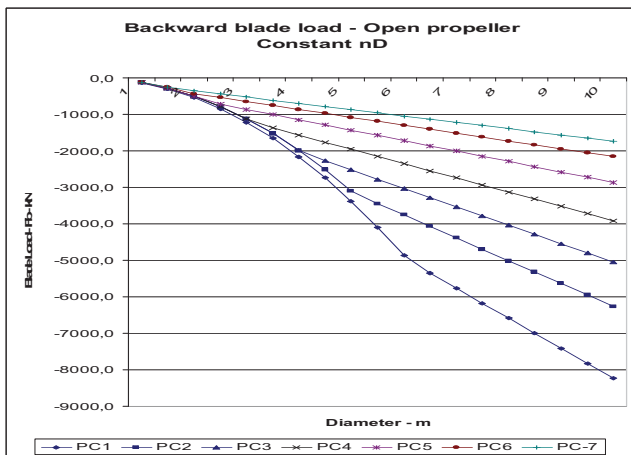


Figure 1 Backward load with parameters $d/D = 0.35$, $nD = 12$, $EAR = 0.7$ and $Z=4$

The most significant parameters are generally Ice Class and propeller diameter.

The product nD at nominal RPM varies little and in practical designs an upper limit normally exists for the avoidance of blade tip cavitations. Significant effect is however seen when the propeller speed drops:

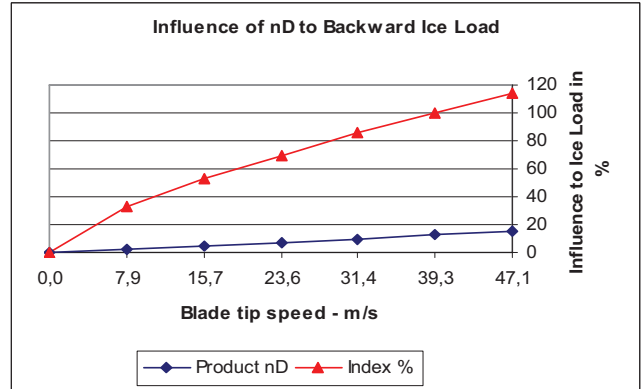


Figure 2 Influence on tip speed on backward ice load

Ratio EAR/Z does not normally vary very much and its influence will be quite small:

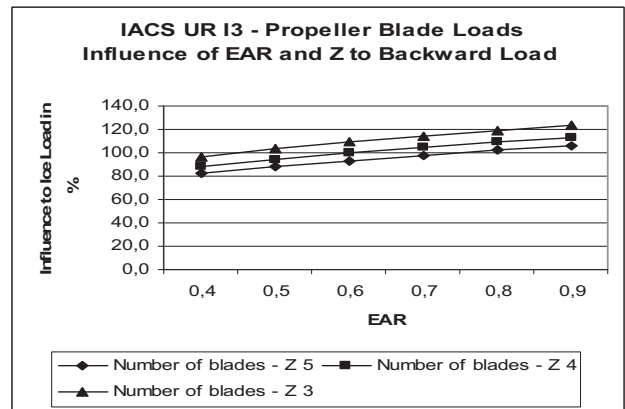


Figure 3 Influence on blade area on backward load

The above show that for any given ice class, and accompanying design ice thickness, the design ice load for small propellers increases with the square of diameter, until D_{limit} is reached. Above D_{limit} , design ice load increases linearly with increasing diameter. Both statements are valid provided that nD is kept constant and EAR/Z is same

2.2 Maximum forward blade force

The forward blade load on the open propeller is a non-contact load occurring due to the very close proximity of an ice block and propeller blade. These loads have been measured directly [Reference 9], but the exact mechanism of their generation and the shape of the load distribution on the blade are not fully understood. The formulae for forward blade bending load, F_f (kN) in regulation section I3.4.3.2 (“IACS (2006)”), model the available full scale information.

When $D < D_{limit} = 2/(1-d/D) H_{ice}$:

$$F_f = 250 \left(\frac{EAR}{Z} \right) D^2 \quad (4)$$

When $D > D_{limit}$:

$$F_f = 500 H_{ice} \left(\frac{EAR}{Z} \right) \left(\frac{D}{1 - d/D} \right) \quad (5)$$

Where d is hub diameter (m).

At any given propeller diameter, the forward blade load increases with ice thickness, until ice thickness equals blade length and one whole blade at any time can be shielded by the ice block.

These loads are to be applied following the same scheme as for the full milling backward blade loads, except that the loads are applied to the face (pressure) side of the blade.

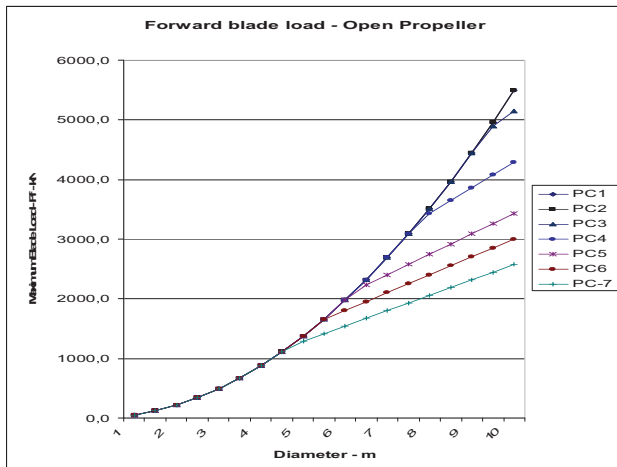


Figure 1 Forward load with parameters $d/D = 0.35$, $nD = 12$, $EAR = 0.7$ and $Z=4$

2.3 Maximum blade tip force

For open propellers, full-scale experience indicates that loads acting over the tip area also occur (“Koskinen & Jussila (1991)”, and DNV damage investigations from 1983-1990). These tip loads may bend the blade backwards when the vessel is going ahead, for example when a ship is turning, and an ice block enters the propeller in the radial direction.

Forward blade tip bending loads also occur. Whereas their magnitude is reasonably well defined, their nature and exact location are not as well understood as for the backward bending loads.

Investigations have shown that 50% of backward and forward blade bending force may be representative for the magnitude of backward tip bending force and forward tip bending force, respectively. The load model should have homogenous pressure distributed over the blade surface outside the $0.9R$ radius on the face (suction) side for the backward force. Similar applies on the back (pressure) side for the forward force.

This tip load is only relevant for static blade strength and will often be dimensioning the outer radii of open, highly skewed, CP propellers.

For ducted propeller, the tip region will to some extent be protected against ice impact loads, and hence this load scenario is not considered relevant.

2.4 Maximum trailing edge force

During winter 2003 DNV experienced several damages on moderately skewed FP propellers, caused by propeller – ice interaction, most likely during reversed operation in ice condition. In all cases, the blade tips on the trailing edge side were bent backwards.

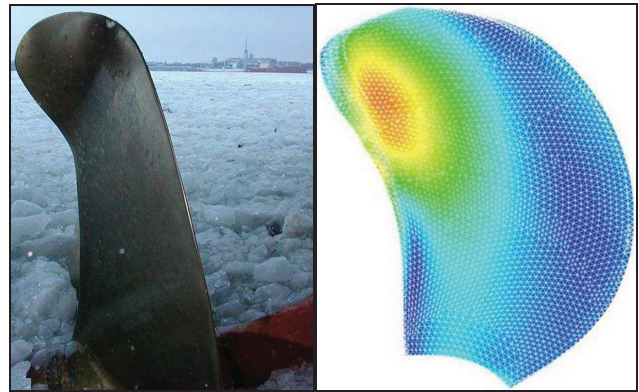


Figure 5 Bent blade and corresponding FE model

Investigations including finite element calculation using a variety of possible loads and pressure distributions were carried out in order to model ice loads corresponding to the damages observed. It was found that for reversible propellers, a trailing edge load with a magnitude of 60% of maximum forward or backward blade bending load (whichever is the largest) was relevant. Representing the ice load by homogenous pressure on the face (suction side) acting radially from $0.6R$ to the tip, and with a chord-wise distribution of 20% of the chord length forward from trailing edge, the observed damages could be fairly re-calculated numerically.

This tip load case is only applicable for static blade strength of reversible propellers and will often be dimensioning the outer radii of open, skewed, FP propellers.

3 ICE LOAD MODELS

The JRPA#6 three-dimensional numerical simulation model was developed by the mid-1990’s, and was used to determine parametric influences upon propeller and ice interaction loads. These loads applied to open propellers and included backward blade bending moment, blade spindle torque, propeller torque and shaft thrust.

Included in the load formulae was the parameter of blade attack angle. The exact value of this parameter is not known at the time of maximum load and it was therefore necessary to make a final calibration of the formulae using

all available full scale data. A design interaction blade attack angle of + 4 degrees was adopted.

4 STATISTICAL REPRESENTATION OF ICE LOADS

The full scale observations and measurements and laboratory tests mentioned in Ch. 2.1 indicated that the ice impact loads on the blade followed a Weibull probability distribution, with a shape factor $K = 0.75$ and 1.0 for open and ducted propeller, respectively. This is however valid for the blade bending loads only. For ice torque open and ducted propellers shall be considered equally. This probability is described as follows:

$$P\left(\frac{F_{ice}}{(F_{ice})_{max}} \geq \frac{F}{(F_{ice})_{max}}\right) = \left(e^{-\left(\frac{F}{(F_{ice})_{max}}\right)^K \ln(N_{ice})}\right) \quad (6)$$

For simplification purposes K could be taken as 1.0 also for open propeller bending loads, although this is slightly conservative. Hence, the Weibull probability distribution will be reduced to one exponential distribution. The probability of a random ice load, F_{ice} (kN) exceeding a given load level, F (kN) is then described as a function of the maximum ice load during life time, $(F_{ice})_{max}$, or ice torque $(Q_{ice})_{max}$ and number of total ice impact loads, N_{ice} .

5 STRENGTH ASSESSMENT OF ESSENTIAL PROPELLER COMPONENTS

5.1 Strength Assessment In General

Essential parts of the propeller should be assessed with respect to both extreme (static) loads as well as dynamic (fatigue) loads. Additionally, the selective strength principle applies, i.e. parts in the propeller / propulsion line should not be damaged in case the propeller blade is bent due to an (unforeseen) excessive ice impact load.

The propeller/ice impact loads are described in previous sections.

All stresses referred to are equivalent stresses for static analysis and principal stresses for fatigue analysis, unless otherwise is specified.

5.2 Propeller Blades

Currently, no analytical calculation method has been found to be sufficiently accurate to predict the propeller blade stresses when exposed to the defined ice loads, except for the root section. Hence, strength assessment of entire propeller blades should be carried out on basis of finite element calculations.

5.2.1 Static loads and strength

When exposed to “once in a life time” loads as described in the ice force chapters, the propeller blades shall not be significantly damaged. Thus calculated stress shall not exceed the material reference stress, σ_{ref} (N/mm^2), applying a safety factor of 1.5 . The reference stress is limited by the lowest of $0.7\sigma_u$ or $0.4\sigma_u + 0.6\sigma_{0.2}$, where σ_u is tensile

strength (N/mm^2) and $\sigma_{0.2}$ is yield strength (N/mm^2) of material.

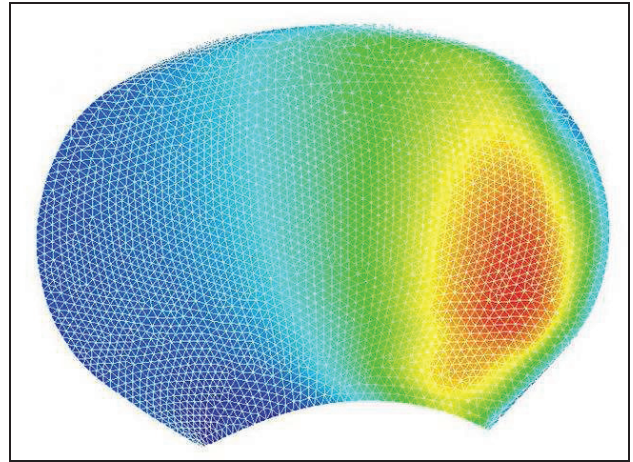


Figure 6 Stresses for load case No. 1 (leading edge load)

Similar calculations should be carried out for all of the relevant load scenarios and stresses to be compared to the reference stress as mentioned above. Calculated stresses at any blade location shall not exceed $\sigma_{ref}/1.5$ in any of the static load cases.

5.2.2 Dynamic loads and strength

Maximum dynamic stress range, $\Delta\sigma_{max}$ (N/mm^2) may be defined as the difference in stress when exposed to maximum backward load (load case 1) and maximum forward load (load case 3) And the stress amplitude $\sigma_{a,max} = \Delta\sigma_{max}/2$ (N/mm^2). This corresponds to the “once in a life time” load situation. Further, the stress range/amplitude distribution is assumed to follow a linear reduction vs. the logarithm of number of cycles. Mean stress, σ_{mean} (N/mm^2) should be taken as mean stress due to hydrodynamic propeller load in ice condition.

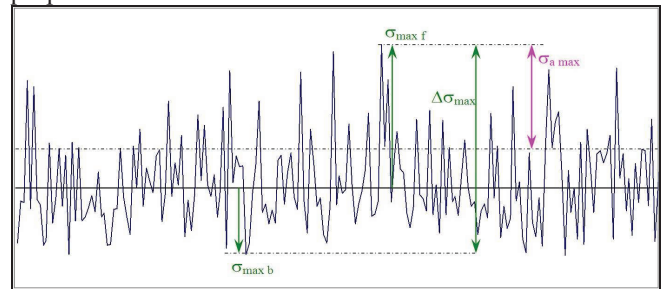


Figure 7 Time series of blade stresses

The above is a simplification, since the number of cycles related to backward and forward blade load is not necessarily the same. However due to the conservatism built into the calculation method in total, results should be on the safe side.

Sufficient fatigue strength vs. dynamic loads should be documented by means of a cumulative fatigue calculation, according to Miner’s rule. Investigations have shown that

dividing the stress spectrum into $I = 10$ blocks, chosen as given below will give a sufficient accuracy:

Stress amplitude for block No. i :

$$\sigma_i = \sigma_{a \max} \left(1 - \frac{i-1}{I}\right) \quad (7)$$

No. of cycles in block No. i :

$$n_i = N_{ice} \left(\frac{i}{I}\right) - \sum_{i=1}^i n_{i-1} \quad (8)$$

Where N_{ice} is the number of ice impacts (-) experienced by the propeller blade during its life time, as defined in "IACS UR I3 (2006)". The formulation is conservative, because each block refers to the nearest load level above.

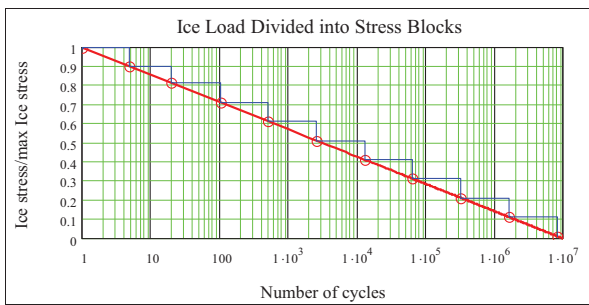


Figure 8 Example of ice loads versus number

Miners rule sum up damage fractions, n_i / N_i , where N_i is allowable number of cycles for the load level (stress block) in question (according to the material SN diagram – see below). Hence the total fatigue damage is given by the Miner sum, D (-):

$$D = \sum_{i=1}^i \frac{n_i}{N_i} \quad (9)$$

A Miner sum, $D < 1.0$ is sufficient, since safety factors are included in the values for fatigue strength (see below), and load level for each block is chosen conservatively.

Material fatigue strength is a function of the number of load cycles. Between the defined points, the curves are linear in a log – log diagram. Fatigue properties (including safety factor 1.5) are proposed to be taken as follows (including the effect of variable loading on fatigue strength by extending fatigue curve with slope 4.5 from 10^7 cycles to 10^8 cycles):

$$N_i = 10^7 \text{ cycles} : \sigma_{E7} = \frac{K_{size} K_{mean} \sigma_{Fat E7}}{1.5} \quad (10)$$

$$N_i < 10^8 \text{ cycles} : \sigma_{Ei} = \sigma_{E7} \left(\frac{10^7}{N_i}\right)^{1/4.5} \quad (11)$$

$$N_i \geq 10^8 \text{ cycles} : \sigma_{Ei} = \sigma_{E8} \left(\frac{10^8}{N_i}\right)^{1/10} \quad (12)$$

Where $\sigma_{Fat E7}$ (N/mm^2) represents fatigue strength from testing (10^7 cycles in sea water – 50% survival probability). K_{mean} is a reduction factor (-) including effect of mean

stress (see below) and K_{size} is a factor (-) taking into account the influence of size effect, as given for K_{thick} in the DNV classification Notes 41.5 (2007), § 2.3.

On basis of work carried out “by Wenshot (1986)”, the mean stress influence is taken as follows for bronze materials:

$$K_{mean} = 1.0 - \left(\frac{1.4 \sigma_{mean}}{\sigma_u}\right)^{0.75} \quad (13)$$

Tests carried out “by Maining et al (1973)”. shows that for stainless steels, the Goodman formulation represents the influence of mean stress quite well. Hence for stainless steel materials the following applies:

$$K_{mean} = 1.0 - \frac{\sigma_{mean}}{\sigma_u} \quad (14)$$

The above is to some extent contradictory to present rule formulations, see DNV rules Pt.4 Ch.5 Sec.1 table B1 (2009), and may call for a rule revision.

Materials fatigue endurance has been investigated by testing for most commonly used materials. However most of those tests were conducted for a long time ago. It is necessary to operate with endurance values reflecting the components actual production methods (casting process, welding, heat treatment etc.), loading patterns (bending vs. tension, shear etc) as well as the materials behavior of changing over time (corrosion etc.).

However, the following values are indicated for the most common propeller blade materials:

Table 2 Indicated fatigue strength for common materials

Material	$\sigma_{Fat E7}$
Ni-Al Bronze (CU3)	127 N/mm^2
12/1 Martensitic stainless steel	120 N/mm^2
13/4 or 13/6 Martensitic stainless steel	130 N/mm^2
16/5 Martensitic stainless steel	140 N/mm^2

5.2.3 Calculation example

Fictive case selected and results are shown in the figure 9.

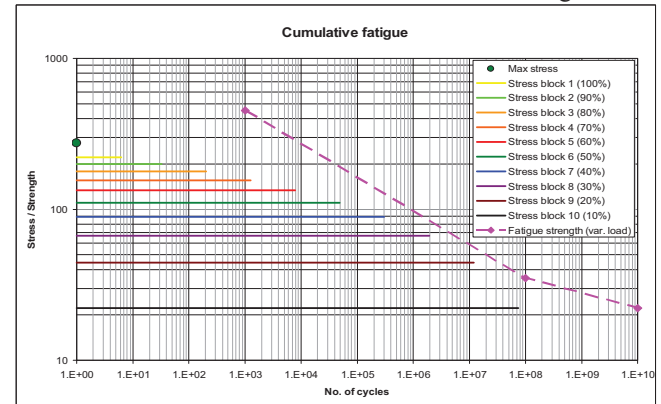


Figure 9 Calculation of static strength and fatigue damage – Miner sum

Material:	NiAlBronze
Yield strength:	270 N/mm ²
Tensile strength:	630 N/mm ²
Number of ice impact loads:	8.8·10 ⁷
Maximum forward stress:	275 N/mm ²
Maximum backward stress:	170 N/mm ²
Thickness of considered section:	100 mm
Fatigue strength (10 ⁷ cycles)	58 N/mm ²

The above example leads to a miner sum of 1.1 (most significant part damages: 0.24, 0.38 and 0.35 from stress blocks 7, 8 and 9, respectively) which means that fatigue strength would not be sufficient. That means that fatigue strength may be dimensioning for propeller blade strength.

It should, however, be mentioned that in the calculation example, a relatively high number of ice cycles has been used.

5.3 Propeller Blade Bolts / Shear pins

5.3.1. Static loads and strength

Blade bolts and shear pins need to withstand the maximum loads caused by propeller–ice impact. However, the required strength criteria is based on selective strength principle, i.e. failure of the propeller blade root section due to an extreme ice load (acting at 0.8R) shall not cause yielding of bolts or shear pins. Safety factor shall be 1.5.

The bolts will carry the propeller bending moment, and for conventional blade bolt arrangements it may be assumed that bending of flanges occurs about an axis being a tangent to the bolt pitch circle.

The bolt pre-stress must be selected to prevent separation of flanges at maximum ice load ($F_{ice,max}$).

The shear pins will carry the spindle torque, subtracted the friction torque between the flanges (caused by the bolt clamping) and friction torque from the blade bearings.

5.3.2. Dynamic loads and strength

Currently, it has not been considered necessary to include fatigue as an additional design criterion for ice loads on bolts and shear pins.

5.4 Propeller Hub and pitch mechanism

Strength of hub and pitch mechanism may be documented by means of finite element calculations. However, such will in general be quite comprehensive, because a FE model needs to include detailed geometry of all parts, including fillets and other stress risers. Further, wide use of contact elements would be needed to describe the load transmission correctly.

Analytical stress calculations may be used, but there are some challenges related to internal load modeling and stress calculations. Some of these are discussed below.

5.4.1 Static loads and strength

The hub and the parts of the pitch mechanism should comply with the same requirements for static strength as the blade bolts and the shear pins, i.e. a safety factor of 1.5 should be documented against yielding when exposed to maximum ice loads and blade failure. When considering static loads, the effects of local stress-risers may be neglected.

The bending moment from the propeller-ice interaction is assumed to be taken up by the blade bearings, and for the pitch mechanism, loads related to ice-interaction will only be generated from blade spindle torque and servo forces.

5.4.2. Dynamic loads and strength

There will be locations at the components in the hub and pitch mechanism where stresses are significantly higher than in the surrounding material. These stress risers, such as notches or fillets forming the transition between different shapes, are critical w.r.t. fatigue strength. In case such local stresses at maximum load exceeds $\sigma_{0.2}$ or $0.7\sigma_u$, cumulative fatigue calculations should be carried out.

The spindle torque variation spectrum also follows a linear distribution vs. the logarithm of number of cycles. As mentioned below, the relation between load and stress in the pitch mechanism components is not strictly linear. However, fatigue damage will mostly accumulate at the lower load levels / higher load cycles. Further, the deduction in torque caused by friction in the bearing is also depending on the load. Hence, a linear relation between load and stress may be assumed as a simplification, and fatigue stress amplitude for block No. i may be written:

$$\sigma_i = \left(1 + f_{rough} + q(K_t - 1)\right) \sigma_{a,max} \left(1 - \frac{i-1}{I}\right) \quad (15)$$

Where f_{rough} is influence factor for influence of surface roughness (-), q equals the notch sensitivity factor (-), and K_t is the *geometrical* stress concentration factor (-).

The influence factor for surface roughness may be derived from DNV classification notes 41.4, § 4.4.4, i.e:

$$f_{rough} = \frac{\sigma_u - 200}{2500} (0.8 + \log Ra) \quad (16)$$

Where Ra is surface roughness (μm).

For steel materials, notch sensitivity factors, q are widely described in literature as functions of notch radius and material strength, for instance “by Shigley et. al (2001)” or by “Agerman (1960)”

Bronze materials have in general lower notch sensitivity than steel. Some sources, such as “Grover (1956)” even indicate a value of zero (no influence of notch on fatigue strength) for bronze.

It should be noted that results presented in literature on notch sensitivity are somewhat ambiguous. Hence, this topic needs further investigations. To be on the safe side, it is recommended to use similar formulations for bronze

materials as for steels, until fairly reliable formulations are found.

Notch sensitivity factors mentioned in literature refer to high cycle fatigue, i.e. $> 10^6$. For lower number of cycles linear interpolation in the log diagram may be applied.

Geometrical stress concentration factors, K_t may also be predicted from literature, such as “Peterson (1974)”. However, FE calculations indicate that some corrections may be necessary, see below.

Fatigue strength for components in pitch mechanism is influenced by a number of effects. In general, the following applies for fatigue strength at E_i number of cycles:

$$\sigma_{E_i} = \frac{\sigma_{fatE_i}}{1.5} K_{mean} K_{size} K_{var} K_{load} \quad (17)$$

Where σ_{fatE_i} is fatigue strength in rotating bending for un-notched test piece, K_{mean} is correction factor for influence of mean stress, K_{size} is correction factor for influence of size, K_{var} is correction factor for influence of variable loading and K_{load} is correction factor for other type of loading than bending.

Fatigue strength for materials relevant for application in hubs and pitch mechanisms for propellers with ice class are widely described in literature, however with somewhat ambiguous results. The following fatigue strength values are indicated ($\sigma_{Fat E7}$ is fatigue strength at 10^7 cycles (N/mm^2)):

Table 3 Indicated fatigue strength for common materials

Material	$\sigma_{Fat E7}$	Slope, x
Bronze alloy	$0.3 \sigma_u$	8
Cast steel	$0.4 \sigma_u$	10
Forged and rolled steel	$0.5 \sigma_u$	15

$$N_i < 10^8 \text{ cycles} : \sigma_{Fat E_i} = \sigma_{Fat E7} \left(\frac{10^7}{N_i} \right)^{1/x} \quad (18)$$

$$N_i \geq 10^8 \text{ cycles} : \sigma_{Fat E_i} = \sigma_{Fat E8} \left(\frac{10^8}{N_i} \right)^{1/50} \quad (19)$$

(Nodular cast iron is normally not relevant because of too low Charpy-V impact strength - min. 20J at $-10^\circ C$, as required by “IACS (2006)”).

The effect of variable loading on fatigue strength is included by extending fatigue curve with low slope (x) from 10^7 cycles to 10^8 cycles. Hence K_{var} is 1.0.

K_{mean} can be found according to the Goodman formulation, see equation No. (14).

For bronze and cast steel, K_{size} valid for 10^7 or more, can be found according to the following formulation as derived from “Valøen (1989)” using a representative thickness / diameter of the loaded part of the component as reference for size, t :

$$K_{size} = 1 - 0.12 \ln \left(\frac{t}{25} \right) \quad (20)$$

For 10^3 cycles or less $K_{size} = 1.0$, and for intermediate number of cycles, interpolated values ($\log N$) may be used.

For forged steel, K_{size} is closely connected to mechanical properties and may thus be taken as 1.0.

In case the loading on the component considered is not dominated by bending, this should be compensated for.

In case of axial stresses (such as for pull-push rod) K_{load} may be taken as 0.85 when number of cycles exceeds some 10^7 . For lower number of cycles than 10^7 : same approach as for notch sensitivity.

In case of shear stresses K_{load} should be taken as $\frac{1}{\sqrt{3}}$ over the whole cycle range.

Note that type of loading also influences on other factors found from literature, mainly geometrical stress concentration factor.

5.4.3 Design servo pressure

The servo system should be designed for the extreme pressures that may occur due to ice load (spindle torque – minus friction torque) on one blade, including blade bending load.

5.4.4 Servo cylinder

The servo cylinder should (if located in the propeller hub) be designed according to criteria for pressurized cylindrical shells / dished ends as given in DNV rules Pt.4 Ch.7 Sec.4 C (2009). Design pressure should be taken as given above, and nominal design stress as $\sigma_{0.2} / 1.5$.

5.4.5 Blade bearing

The blade bearings, are considered the most critical location in the propeller hub itself w.r.t. ice strengthening. The bearings should be checked for:

Max ice loads and blade failure load:

- Maximum surface pressure (no yielding)
- Maximum nominal bending stress ($\max \sigma_{0.2} / 1.5$)

Dynamic ice loads:

- Fatigue stress (bending) in fillet and/or notch / groove

In addition to the loading from propeller-ice interaction, the mean centrifugal force on propeller blade should be included.

Special attention should be paid to the blade sealing arrangement, avoiding sharp notches in O-ring grooves in way of highly stressed areas. Similar also applies for the bearing surfaces on blade flange and crank disk.

Both when calculating surface pressure and bending stresses, it should be taken into account that the bending moment, M_b from the propeller-ice interaction load will cause an uneven pressure distribution over the bearing surface. Assuming the pressure to have a sinus distribution

around the periphery, and the boring diameter, D_b of the blade bearing to be much larger than the breadth, b of the bearing surface, the following pressure contribution from the ice load is found at the highest loaded area.

$$p = \frac{\pi M_b}{b(D_b + b)^2} \quad (21)$$

The above expression does not account for the influence of deflections, which is on the conservative side.

Local bending stresses may, as a simplification, be calculated from the above pressure, using strip-theory.

5.4.6 Internal load transmission in pitch mechanism

The following addresses cross-head type of pitch mechanism, whereas other methods for load transmission are also possible and well-known.

A non-linear relation between loads and stresses is introduced due to an increasing degree of deflections in the mechanism and hub with increasing load level. This applies in particular for the crank pin and retaining wall for sliding block. This is illustrated below, where it can be understood that as load and deflections increase, the contact pressure will shift from a uniform distribution towards the “root” of the crank pin and the “top” of the retaining wall (because the crank pin normally deflects more than the retaining wall).

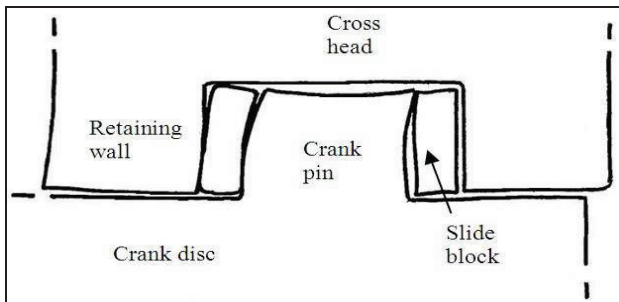


Figure 10 Illustration of component deflections

Similarly, high contact pressures will cause compression of the surfaces of crank pin and retaining wall, as well as the slide block. This will lead to a concentration of the stresses in way of the centre line of the pressurized area. This is indicated below:

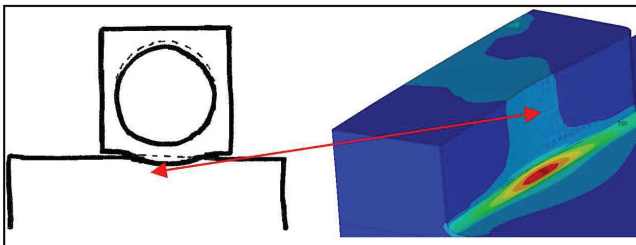


Figure 11 Illustration of surface deflections of retaining wall

The pitch mechanism will be exposed to ice loads with the propeller pitch in various positions. This will also introduce a non-linear dependency between spindle torque and loads

on parts in the pitch mechanism. Further, in particular for the retaining wall, maximum stresses will occur at different locations along the wall, depending on propeller pitch.

The propeller ice loads are however dominated by the ice condition going ahead with high power and low ship speed. For simplicity, calculations may hence be carried out with propeller pitch corresponding to 70% of the MCR ahead pitch for all ice load conditions.

5.4.7 Stress calculation for crank pin

Stress calculations for the crank pin should be carried out for the same conditions as for the blade bearing.

When deflections can be neglected (low load) an even height-wise load distribution may be assumed for the crank pin (i.e. point of attack is half way up the crank pin). Finite element calculations indicate that at higher load (when deflections become more significant) pressure distribution normally shifts towards a triangular height-wise distribution, with point of attack shifting down to 1/3 up the crank pin for relatively rigid retaining wall (note that this shift is non-conservative calculation-wise).

Because of the relative low height / diameter ratio of the crank pin, corrections should be applied if stresses are calculated analytically according to cantilever beam theory.

Similarly, additional stress concentrations due to local compression of the surfaces should be included, in particular at high loads.

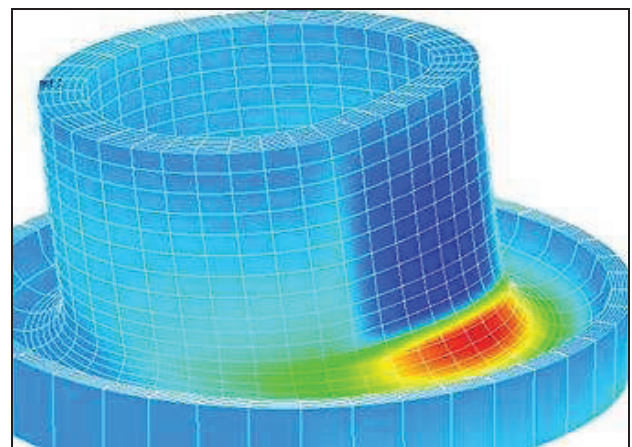


Figure 12 Stress and local compression of crank pin

This will influence on the fatigue calculations, although mostly at low-cycle (large loads / deflections). Comparison with finite element calculations for a high load situation indicates that cantilever beam calculations incorporating geometrical stress concentrations as found from “Peterson (1974), fig. 189” for short beam with shoulder (extrapolated), underestimate local stresses in crank pin with a factor of some 1.3 (depending on clearance to sliding block).

Further work is needed, in order to determine and account for the influence of the local, hemispherical stress

concentration and to differentiate it from the effects of shortcomings of the cantilever-beam theory for short beams. “Peterson (1974), fig. 189” results also indicate that stress concentration on tension side and compression side is fairly the same (slightly higher on compression side), i.e. a direct relation between reversed stresses and reversed loads is a fair assumption.

For the crank pin, maximum load amplitude should hence be taken as the average value of forward and backwards ice spindle torque

In the same way as for propeller blades, the mean load on crank pin may as a simplification be taken as servo force necessary to keep the blade in position due to hydrodynamic and centrifugal loads on blade.

5.4.8 Stress calculation for slide block

The slide block is mainly loaded in compression, and normally without significant stress risers. Further, the slide block is normally made of softer material than crank pin and/or retaining wall. Hence, only a static consideration is necessary. If nominal surface pressure on projected area during extreme load does not exceed yield strength of material, the slide block strength is sufficient.

5.4.9 Stress calculation for retaining wall

Stress calculations for the retaining wall should be carried out for the same conditions as for the blade bearing and crank pin. Also, similar to as for the crank pin, the loading distribution on the retaining wall to some extent depends on load level and corresponding deflections. At low load, point of attack may be assumed to be half way up the wall. Approaching a triangular load distribution at high load, point of attack will normally shift towards the top end. Up to 2/3 of the height may be representative point of attack for a relatively rigid retaining wall (this shift is in general in conservative direction, calculation-wise).

Regarding local stress concentration in way of the pressure centre axis, the “footprint” of the crank pin can be seen on the retaining wall. Hence increased stress in way of pressure centre axis is also seen for retaining wall.

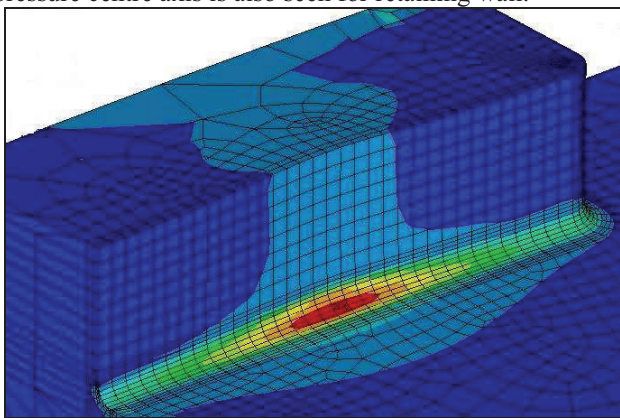


Figure 13 Stress and local compression of retaining wall

For analytical calculations, it is found from comparison with Finite Element calculations that effective load carrying breadth of retaining wall can be taken as breadth of sliding block when it comes to static strength, whereas a breadth corresponding to the crank pin diameter seems to be relevant for fatigue calculations – taking the local “focused” stress concentration into account.

Using stress concentration factors as from “Peterson (1974), fig 189” for short beam with shoulder (extrapolated when necessary), the stress prediction is expected to be reasonable, both in fillet as well as nominal stresses.

Neglecting the influence of the shift in location for peak stress along the fillet as pitch changes (different location of slide block vs. retaining wall), the fatigue calculation will be somewhat conservative when it comes to number of cycles.

Each retaining wall will only take load in one direction. Hence dynamic stresses will go from zero to max ($R=0$). Stress amplitude and mean stress may hence be taken as average of load due to ice spindle torque (backward or forward bending) plus load necessary to keep the blade in position due to hydrodynamic and centrifugal loads on blade.

5.4.10 Stress calculation for push - pull rod

Stress calculations for the push-pull rod should be carried out for the same conditions as for the blade bearing, crank pin and retaining wall.

Loading may normally be considered as purely axial. That is unless the push-pull rod also acts as a journal bearing inside the hub (normally undesirable for high ice class), which will cause bending of rod due to eccentric loading on crosshead when ice spindle torque is acting on one blade.

Maximum static stress is hence found as axial stress in section with minimum diameter, whereas fatigue should be considered at any stress riser such as fillets or radial borings.

Special attention to fatigue strength is also to be paid to welded connections, where the weld will cause a significant reduction in material fatigue strength.

6 CONSEQUENCES FOR MANUFACTURERS OF PROPULSION SYSTEMS

The recently presented rules for Polar Class and Finnish-Swedish Ice Classes are requiring considerable efforts for interpretations by manufacturers for propulsion systems and by the classification societies.

DNV wants to be proactive and cooperative increasing competence through discussions, workshops and case studies.

The manufacturers continuously facing the market requesting “their” system to fulfill all possible new

requirements is of course a driver for development of new systems for project based calculations and dimensioning of propulsors to the new ice class rules. This requires deep knowledge of the rule requirements and an iterative approach to reach the constraints for the product portfolio.

Due to that the rules require deep analysis of both propeller and shafting system is it necessary to execute several steps of iterations before a solution is reached. This is time consuming and therefore is it necessary to create tools for interpretations and simplifications of the final design verification step.

The most rules have until today focused on the propeller blades and a static pyramid (visualized) strength of the propeller hub. The IACS UR I3 (2006) and the Finnish-Swedish Ice Class Rules (2008) are requesting the CP-mechanism to be assessed with respect to both static and dynamic loads. However applicable loads and permissible stresses are defined only and the strength assessment is left to the discretion of the respective classification society.

There are indications that in the most cases the static criterions for the propeller blade and the aft part of the propeller shaft will be the dimensioning factor. However for the CP-Mechanism will it still be beneficial to relate to cumulative fatigue analyzes. DNV is striving for clearer definitions of the requirements for the CP-Mechanism in coming rules and supporting documents.

To verify compliance with the new requirements it will be necessary to increase the documentation extent to cover the whole scope. It will likely be necessary to have detailed calculations from the manufacturers and the assessments' will require far more details than just power, rpm etc. that will call for a closer interaction between classification society and manufacturer. In such process it is beneficial that also involved classification society has good knowledge and understanding on both propulsors and the rules and their background.

REFERENCES

- 1 Agerman, E., (1960) Notch Sensitivity in Steel, Acte Polyt. Scand., Me 8.
- 2 Det Norske Veritas (2007) 'Calculation of Marine Propellers' DNV Classification Notes 41.5.
- 3 Det Norske Veritas (2009) 'Boilers, Pressure Vessels, Thermal-oil Installations and Incinerators' DNV Rules for Ships, High Speed / Light Craft and Naval Surface Craft, Pt.4 Ch.7 Sec.4.
- 4 Det Norske Veritas (2009) 'Rotating Machinery, Driven Units' DNV Rules for Ships, High Speed / Light Craft and Naval Surface Craft, Pt.4 Ch.5 Sec.1.
- 5 Finnish Maritime Administration (2008), 'Finnish-Swedish Ice Class Rules'.
- 6 Grover et al. E.,(1956) Fatigue of Metals and Structures, Thames and Hudson, London UK.
- 7 IACS (Jan 2007) 'Machinery Requirements for Polar Class Ships', IACS Unified Requirements I3.
- 8 IACS Unified Requirements for Polar Ships, Background Notes to Propeller Ice Interaction Loads (Rev. 2 draft) by Robin Browne and Lasse Norhamo
- 9 JRPA#6 CANADA/FINLAND JOINT RESEARCH PROJECT ARRANGEMENT
- 10 Koskinen, P. and Jussila, M. (1991) Long Term Measurements of Ice loads on Propeller Blade of M/S Gudingen, (translated from Finnish), Research Notes 1260, Technical Research Centre, Espoo, Finland.
- 11 Maiining, F., Rist, A., Walter, H., (1973) 'The Corrosion Fatigue Limit of Large Specimens of Constructional Parts from Steel Castings with 13% Content of Chromium', 40th International Foundry Congress, Moscow, Russia.
- 12 Peterson, R.E., (1974) Stress Concentration Factors, John Wiley & Sons, New York, US
- 13 Shigley, E., Mischke, C.R., (2001) Mechanical Engineering Design, McGraw-Hill, New York, US, pp 386-389.
- 14 Valøen, Å. (1989) Maskindeler, Tapir Forlag, Trondheim, Norway.
- 15 Wenshot, P. (1986) 'The Properties of Ni-Al Bronze Sand Cast Ship Propellers in Relation to the Section Thickness, Naval Engineers Journal, pp 58-69.